Chinese Journal of
POLYMER SCIENCE

RESEARCH ARTICLE

https://doi.org/10.1007/s10118-024-3105-9
Chinese J. Polym. Sci. **2024**, *42*, 1341–1352

Structural Properties of Ions and Polyelectrolytes in Aqueous Solutions under External Electric Fields: The Sign Effect

Cheng-Jiang Lin[a,b], Jun-Jun Wang[c], Yuan Jiang[a], Shu-Li Chen[c], Hong-Fei Li[a,b*], Wen-Han Zhao[c], Qing-Rong Huang[e], Chang-Ru Rong[c*], and Xiao-Zheng Duan[a,b,d*]

[a] *State Key Laboratory of Polymer Physics and Chemistry, Changchun Institute of Applied Chemistry, Chinese Academy of Sciences, Changchun 130022, China*
[b] *School of Applied Chemistry and Engineering, University of Science and Technology of China, Hefei 230026, China*
[c] *National Key Laboratory of Advanced Vehicle Integration and Control, China FAW Group Co., Ltd., Changchun 130013, China*
[d] *State Key Laboratory of Molecular Engineering of Polymers, Department of Macromolecular Science, Fudan University, Shanghai 200438, China*
[e] *Department of Food Science, Rutgers University, 65 Dudley Road, New Brunswick, New Jersey 08901, USA*

Electronic Supplementary Information

Abstract We utilize molecular dynamics simulations to investigate the microstructures of ions and polyelectrolytes in aqueous solutions under external electric fields. By focusing on the multi-body interactions between ionic components and H_2O molecules, as well as their responses to the external electric fields, we clarify several nontrivial molecular features of the ionic and polyelectrolyte solutions, such as the solvations of cations and anions, clustering of the ions, and dispersions/aggregations of polyelectrolyte chains, as well as the corresponding responses of H_2O molecules in these contexts. Our simulations illustrate the variations in structures of ionic solutions caused by reversing the charge sign of the ions, and elucidate the disparity in structures between anionic and cationic polyelectrolyte solutions in the presence of the external electric fields. This work clarifies the mechanism for the alternations in complex multi-body interactions in aqueous solutions caused by the application electric field, which can contribute to the fundamental understanding of the physical and chemical natures of ion-containing and charged polymeric systems.

Keywords Polyelectrolyte; Ions; Aqueous solutions; External electric fields; Asymmetric dipole

Citation: Lin, C. J.; Wang, J. J.; Jiang, Y.; Chen, S. L.; Li, H. F.; Zhao, W. H.; Huang, Q. R.; Rong, C. R.; Duan, X. Z. Structural properties of ions and polyelectrolytes in aqueous solutions under external electric fields: the sign effect. *Chinese J. Polym. Sci.* **2024**, *42*, 1341–1352.

INTRODUCTION

Polyelectrolytes (PEs), constituted of repeated ionic monomer units, represent an important class of charged polymers and have attracted extensive attention due to their importance in natural science and industry.[1–4]

Polyelectrolytes usually exhibit ideal solubility in aqueous solutions, and the unique physicochemical properties of polyelectrolyte solutions mainly stem from the intricate multi-body electrostatic interactions among ionic components and dipolar solvents. Specifically, the electrostatic interactions of polyelectrolytes and counterions can cause complex ionic correlations,[5–11] and the water solvent molecules exhibit dipolar natures, which can interact with the polyelectrolytes and ions through the ion solvation effects.[12–18] These two effects naturally couple with each other. On one hand, the superpositioned electrostatic fields of the ionic components can restrict the orientation of the nearby dipolar solvent molecules and change the local dielectric properties of the solutions; on the other hand, the changed local dielectric properties can conversely alter the electrostatic interactions of the correlated ionic groups. Furthermore, the applied electric fields can exert opposite electric forces onto the anionic and cationic species, and result in reorientations of the dipolar solvent molecules and even the dielectric decrement of the systems.[18–22] In this context, the intricate electrostatic interplays between ionic components and dipolar solvent molecules, as well as the physicochemical properties inherent to polyelectrolyte solutions, can be significantly altered.

In recent decades, extensive theoretical studies, simulations and experiments have been employed to explore charged and ion-containing polymers and their complexations or coacervations.[22–41] However, modeling the multi-body electrostatic interactions in polyelectrolyte solutions remains challenging. Due to the simplicity and lower computational cost, traditional coarse-grained simulations and theories have been used to study polyelectrolyte solutions. How-

* Corresponding authors, E-mail: hfli@ciac.ac.cn (H.F.L.)
E-mail: rongchangru@faw.com.cn (C.R.R.)
E-mail: xzduan@ciac.ac.cn (X.Z.D.)

Special Issue: Charged Polymers
Received December 28, 2023; Accepted February 20, 2024; Published online April 3, 2024

ever, in these approaches, the solvent molecules are usually treated as a continuous medium with certain dielectric constants, and these manipulations are insufficient to detect the complex multi-body correlations among the charged and polar components, let alone their coupling with the connectivity of polymer chains and external field or complicated surfaces/interfaces. Among others, modeling the dipolar or polar solvent molecules as dipolar coarse-grained particles with variable symmetric dipole moments serves as a robust approach to efficaciously capture the reorientations and reorganizations of the polar solvents in response to the electrostatic fields originating from the ionic groups or external electric fields. For example, He *et al*. developed an improved polarizable model based on Drude oscillator and employed the coarse-grained molecular dynamics (MD) simulations to investigate the structural changes and phase separations of polymer blends and diblock copolymers under the external electric fields.[42,43] Frischknecht *et al*. systematically investigated the role of polarization in the structure and dynamics of ionomer melts by incorporating the Drude oscillator into coarse-grained MD simulations.[44] In the previous study, on the basis of Stockmayer-fluid model, we developed a coarse-grained MD simulation algorithm to study the fundamental physicochemical properties of ionic solutions under the applied electric fields, and systematically explore the multi-body interactions among ions and symmetric dipolar solvents. Moreover, we have utilized this approach to clarify the mechanism for eliminating ionic clusters *via* polar solvent addition in the presence of the electric field, and developed a highly efficient and easy-operating strategy for noise reduction of nanopore technology for detections of charged polymers.[45] In addition, by elucidating the multi-body interplays among ions and dipolar solvents, we revealed the mechanism for multiple phase transitions of dilute solutions of isopolyoxometalate macro-anions and developed novel ionic hydrogels.[46] It is important to note that in these studies, only the symmetric dipolar nature of the liquid molecules is considered; that is, a dipolar particle exhibits equivalent electrostatic interactions with a cation or an anion (if the ionic size and valence are fixed), and the solvation strength of ionic groups is independent of their charge signs. Furthermore, it can be predicted that the statistical structures and dynamics of ionic and polyelectrolyte systems cannot be changed if only the charge signs of the ionic species are reversed, although the multi-body correlations between ions and dipoles are considered.

Nevertheless, the effective dipoles of most polar liquid molecules or chemical groups often exhibit the asymmetric feature, *i.e.*, the position of dipole moment exhibits a shift from the molecular center. These asymmetric dipolar molecules usually show quite distinct affinities to cations and anions, and cause nontrivial disparities in chemical properties between anionic and cationic species. As illustrated by the pioneering theoretical and experimental studies,[47–53] the asymmetric dipolar feature of liquid molecules can cause a significant "sign preference effect" of the ions. In concrete terms, anions can preferentially cause the nucleations of H_2O molecules, whereas cations preferentially induce the nucleations of alcohol-type molecules, due to the reversal orientations and different affinity abilities of these asymmetric dipolar molecules around the cation/anions. Likewise, as demonstrated by our previous study, this sign effect also exists in polyelectrolyte solutions and can result in the qualitatively structural disparity between anionic and cationic polyelectrolytes.[54] Moreover, under the circumstance of applied electric fields, the external electric force exerted on ions and dipolar solvent can significantly alter the multi-body electrostatic interactions, and cause unpredictable variations in the physicochemical properties of ionic and polyelectrolyte solutions. Despite the advance in the theoretical and simulation studies of charged systems, as far as we are aware, the multi-body correlations among ions, polyelectrolytes, and H_2O solvent molecules under the electric fields, as well as the corresponding structures and thermodynamics of ions and polyelectrolytes in the aqueous solutions, remain largely unrevealed.

In this study, we employ molecular dynamics (MD) simulations to investigate the structural properties of ions and polyelectrolytes in aqueous solutions under external electric fields. By focusing on the multi-body interactions among ionic components and H_2O molecules, as well as their responses to the external electric fields, we clarify variations in structures of ions resulting from the charge sign reversion and elucidate the discrepancy in structures between anionic and cationic polyelectrolytes. In section **MODELS AND SIMULATION METHODS**, we concisely introduce the MD model and simulation details. Herein, we couple the coarse-grained model (of ions/polyelectrolytes) and TIP3P model (of water molecules) with the electric forces, to effectively account for the multi-body interplays between ions, polyelectrolytes, the asymmetric dipolar H_2O molecules and their response to the external electric fields. In section **RESULTS AND DISCUSSION**, we first study the orientations of H_2O molecules and solvation effects of single anions/cations in response to the varying electric fields. We then systematically explore several key factors (*i.e.*, the size, charge sign of ions, and electric field strength) on the structures of ionic solutions. Further, we extend our investigation to the polyelectrolytes and illustrate the effects of charge sign, monomer concentration, and electric field strength on the structures of polyelectrolyte solutions. Our study rationalizes the variations in structures in ionic solutions caused by the reversal of the charge sign of the ions, and elucidates the disparities in structures between anionic and cationic polyelectrolyte solutions, under the applied electric fields. In conclusions, we summarize our investigations and provide the concluding remarks.

MODELS AND SIMULATION METHODS

Model

In this subsection, we provide a concise overview of the model and simulation method; more detailed information can be found in our previous publication.[54] Herein, we use MD simulations to explore the solvation effects of single anions/cations in aqueous solutions and the structures of aqueous solutions of ions and anionic/cationic polyelectrolytes under the applied electric fields. To emphasize the impact of the sign effect on the solvations for anionic and cationic species, the TIP3P model is employed to simulate water components, and the coarse-grained model is utilized to simulate ions and PEs (Fig. 1). Notably, all ions and polyelectrolytes in our study are considered to be hydrophilic.

In the TIP3P model of H_2O, each H and O atom takes the

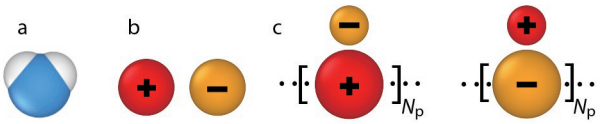

Fig. 1 Schematic illustration of (a) a water molecule (with H in white and O in blue), (b) an anion (in orange) and a cation (in red), (c) a cationic PE chain, an anionic PE chain, and their counterions.

partial charges of +0.415*e* and −0.83*e*, respectively (*e* denotes the elementary charge).[55–57] Based on this model, our simulation can accurately capture the electrostatic response of H_2O molecules toward the neighboring ionic components. Moreover, based on the Dang force field,[58–63] we model each cation and anion as the beads with a positive charge or negative charge at their centers. Since the solvation of ions is primarily influenced by their size,[64,65] a variety of ions (such as Li^+, Na^+, K^+, Cl^-, I^-) of different sizes are considered in the simulations (as shown in Table S1 in the electronic supplementary information, ESI). Additionally, it is essential to compare the distinct mechanisms for solvation of cations and anions with the same other molecular factors but opposite charges; hence, in accordance with the previous work of Koneshan *et al.*,[59] we create the corresponding virtual ions (*i.e.*, Li^-, Na^-, K^-, Cl^+, I^+, Table S1 in ESI). We utilize the bead-spring model to coarse-grain the anionic and cationic PEs composed of N_p=20 connecting (monovalent) monomer beads. The size of each ionic monomer is set to be 4.168 Å, which is equivalent to that of an I^- ion.[66] The size of each counterion is set as 3.25 Å, equivalent to that of K^+. For simplicity, other molecular parameters for each monomer and counterion are determined based on the I^- and K^+ in the Dang force field.[58–63] It should be noted that in the conventional TIP3P model,[55] the size of hydrogen atom is disregarded. To maintain the compatibility between the coarse-grained model (for ions) and TIP3P model, we make modifications to Price's TIP3P model. Specifically, we include the size and energy parameters of hydrogen based on Jorgensen *et al.*'s work when accounting for the ions/H (in H_2O) interactions.[57]

The standard or truncated Lennard-Jones (LJ) potential is utilized to model the nonbonded interactions among all of the aforementioned components,

$$U_{LJ} = \begin{cases} 4\varepsilon_{LJ}\left[\left(\sigma/r_{ij}\right)^{12} - \left(\sigma/r_{ij}\right)^{6}\right] + S, & r_{ij} \leqslant r_c \\ 0, & r_{ij} > r_c \end{cases} \quad (1)$$

Table S1 (in ESI) provides a list of energy parameters (ε_{LJ}) and sizes (σ) of H and O (in H_2O molecules), the chosen ions (both real and virtually generated), and the PE monomers. Lorentz-Berthelot rules ($\varepsilon_{ij} = \sqrt{\varepsilon_i \varepsilon_j}$, $\sigma_{ij} = \left(\sigma_i + \sigma_j\right)/2$) are used to calculate the LJ parameters for species *i* and *j*.[67] *S* is used to shift the LJ potential to 0 at r_c=13 Å, where r_c represents the cutoff. Coulomb interactions are utilized to compute the electrostatic interactions among the partial-charged H and O in H_2O molecules and ionic species,

$$U_{Coul} = \frac{Z_i Z_j e^2}{4\pi\varepsilon_0\varepsilon_r r} \quad (2)$$

where Z_i and Z_j denote the (partial) charge of species *i* and *j*, respectively. We use the PPPM (particle-particle particle-mesh) algorithm to calculate U_{Coul} up to a precision of 10^{-5}.[68] In our model, ε_r=1 and ε_0 represents the vacuum permittivity. Our model employs the harmonic angle potential (Eq. 3) and harmonic bond potential (Eq. 4) to preserve the H_2O structures.

$$U_{Angle} = \kappa_a (\alpha - \alpha_0)^2 \quad (3)$$

$$U_{Bond} = k_b (r - r_0)^2 \quad (4)$$

in which κ_a=55.0 kcal/mol and α_0=104.52°, k_b=450.0 kcal/mol and r_0=0.96 Å.[55–57] The harmonic bond potential is utilized to model the chain connectivity in PEs, in which k_b=29.90 kcal/mol and r_0=4.168 Å. In the simulations, a uniform external electric field ($\vec{E}$) is applied. Herein, the electric force ($\vec{F} = qe\vec{E}$) is exerted along the *x*-axis direction to water molecules, ions and polyelectrolytes. We ignore certain chemical details of the polyelectrolyte and maintain their crucial physicochemical features. This simulation approach can effectively account for the effects of external electric fields and the sign effect of the ionic species.

Simulation Details

Using the Large-scale Atomic/Molecular Massively Parallel Simulator (LAMMPS),[69] we perform MD simulations in the canonical (NVT) ensemble within a cubic box of size L^3. In the simulation, through the introduction of three-dimensional periodic boundary conditions, all particles can interact across the boundaries and can exit from one end of the box and re-enter from the other end. The uniform electric field (applied along the *x*-axis direction) remains independent of periodic boundary conditions. We use the Langevin thermostat to control the simulation temperature as 298 K. The MD time step is to be 2 fs. At the beginning of the simulations, all components are generated randomly within the simulation box. We first study the effect of external electric fields on the solvation of single ions in the aqueous solution. We place a single cation or anion and 1000 water molecules in a box of size *L*=31 Å, and estimate the volume of each water molecule as (3.1 Å)^3. We set the number density of water molecules as ρ_w^*~1.0. For ionic solutions, we conduct simulations in a box with *L*=46.5 Å. We set the ionic concentrations to 0.5 mol/L and fix the number density of ions and H_2O to be 1.0 ($\rho_i^* + \rho_w^* \sim 1.0$). For the PE solutions, we set the simulation box size to be *L*=90.52 Å and vary the amount of PE chains from 10 to 300 (corresponding to a monomer concentration range from 0.45 mol/L to 13.44 mol/L). The highest monomer concentration of 13.44 mol/L corresponds to the chain concentration of 0.672 mol/L, which falls within the commonly used concentration scope in experimental studies.[70] We adjust the number of water molecules accordingly to maintain the number density of 1.0 for all components. In all the simulations, we first conduct 10^6 MD steps (equivalent to 2 ns) to achieve the equilibration of the simulations. We then apply the external electric fields and further perform 10^6 MD steps to achieve the steady state, after which we use another 10^6 MD steps as the production simulation. We vary the strength of the electric field from 0 V/Å to 1 V/Å to analyze the system properties. For each scenario, we conduct numerous simulations with different initial configurations and ultimately generate 10^4 samples.

RESULTS AND DISCUSSION

Solvation of Single Ions in Aqueous Solutions

We first study the orientation of H_2O molecules responding to $\vec{E}$ in pure water (Fig. 2a) and the corresponding radial distribution functions of H atoms surrounding O atoms of H_2O (Fig. 2b). In

Fig. 2(a), α represents the angle between the dipolar vector (connecting O atom and center of two H) of the water molecule and $\vec{E}$. It is worth noting that $<\alpha>/\pi \sim 0.5$ represents the random orientation of H_2O, whereas $<\alpha>/\pi \sim 0$ indicates H_2O orientation parallel to $\vec{E}$. Our simulations indicate that at $E \leq 0.1$ V/Å, the weak external electric forces are insufficient to cause the alignment of H_2O along $\vec{E}$; and therefore, H_2O molecules exhibit random orientation, as shown by the results of $<\alpha>/\pi \sim 0.5$ and the snapshot i in Fig. 2(a). As the external electric field strength increases (E>0.1 V/Å), the H_2O molecules tend to orient along $\vec{E}$, as shown by inset ii in Fig. 2(a), which results in the decay in $<\alpha>/\pi$ (Fig. 2a) and a reduction of peaks in $g_{H\text{-}O}(r)$ (Fig. 2b). Our simulations thus demonstrate that applying strong $\vec{E}$ can lead to significant H_2O orientation and restrict their dipolar responsive ability. Note that the previous theoretical studies have predicted that the dielectric decrement features of liquids can be triggered by strong applied electric fields.[19,71] Our simulations on orientating H_2O along strong $\vec{E}$ clarify the relative molecular mechanism for this effect.

We then explore the effect of $\vec{E}$ on ion solvation in the aqueous solutions. Fig. 3(a) displays the solvation energies for single ions (ΔG) at different radii and electric field strengths. Here, we calculate the solvation energy as $\Delta G = G_{II} - G_{I}$, where G_{II} represents the summation of ion-H_2O and H_2O-H_2O interactions in ion-containing cases, [$G_{II} = U_{i\text{-}w}(II) + U_{w\text{-}w}(II)$], whereas G_I is the H_2O-H_2O interactions in the ion-free case [$G_I = U_{w\text{-}w}(I)$]. Note that $U_{i\text{-}w}(II)$, $U_{w\text{-}w}(II)$, and $U_{w\text{-}w}(I)$ are calculated according to Eqs. (1)–(4). The calculated ΔG for cations and anions can be further defined as ΔG^+ and ΔG^-, respectively. In Fig. 3(b) and Fig. S1 (in ESI), we analyze the orientations of H_2O molecules around a single ion at different $\vec{E}$ by calculating $<\cos\theta>$, where θ represents the angle intersected by the dipolar vector of an H_2O molecule and position vector connecting the dipole and ion. $<\cos\theta> \sim 0$ represents random arrangement of H_2O molecules, whereas $|<\cos\theta>| \sim 1.0$ indicates completely oriented H_2O molecular structures around the ion.

Our simulations illustrate that under the weak electric field E=0.01 V/Å, due to the sign effect of ions solvated by H_2O (of asymmetric dipoles), anions exhibit much smaller solvation energies than cations (Fig. 3a). In this scenario, the ion-water interactions dominate the solvation process. The H_2O molecules show much more apparent affinity to anions and more significant corresponding orientation (Fig. 3b); and with increasing the ionic size, $|\Delta G^+ - \Delta G^-|$ exhibits a decrease, which is due to the weakened H_2O orientation and ion solva-

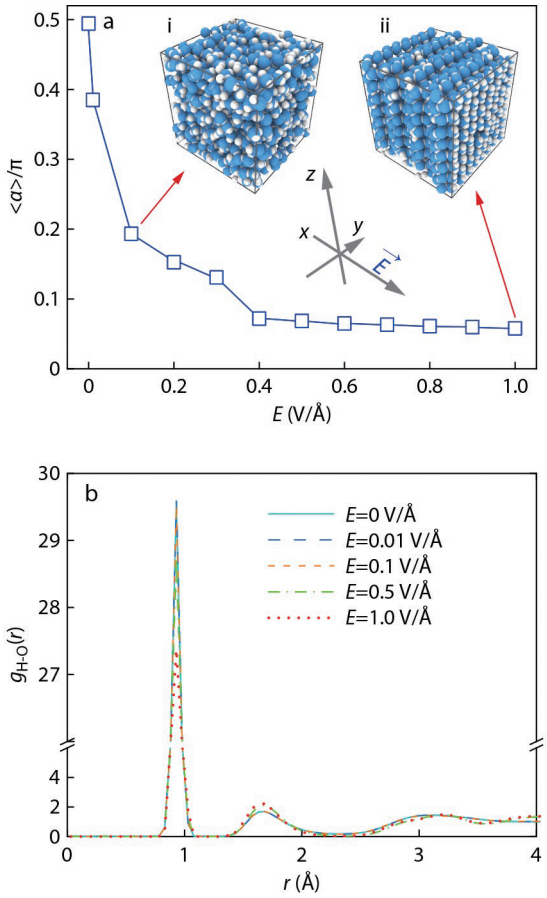

Fig. 2 (a) Average orientations of water molecules at different external electric field strengths, in which (i) and (ii) depict typical snapshots at E = 0.1 and 1 V/Å, respectively; (b) Radial distribution functions of H atoms surrounding O atoms of water molecules.

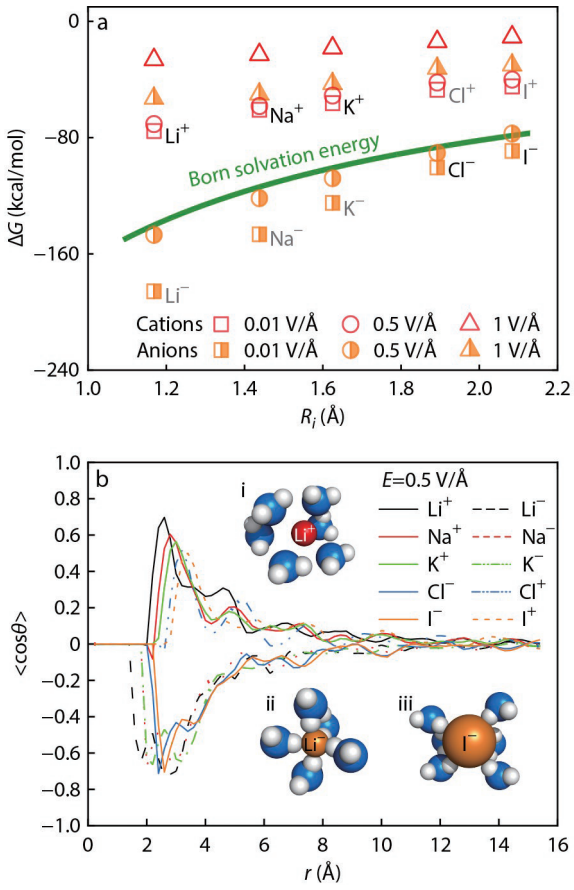

Fig. 3 (a) Solvation energies for single ions at different radii in water under external electric fields. The squares, circles, and triangles represent E = 0.01, 0.5 and 1 V/Å, respectively, and the line represents the Born solvation energy. (b) Orientations of water molecules near single ions under an external electric field strength of E=0.5 V/Å. (i–iii) Indicate the typical H_2O structures around Li^+, Li^-, and I^-.

https://doi.org/10.1007/s10118-024-3105-9

tion. Further, our simulation demonstrates that the enhancement in electric field strength can cause significant alterations in ion solvation. Specifically, the electric field results in the alignment of H_2O molecules along $\vec{E}$, and the dipolar H_2O molecules cannot sufficiently orient around the ions (Fig. 3b), which reduces the solvation effects for single ions. In this context, the sign effect becomes weak and the difference in ΔG for cations and anions exhibits a decrease (Fig. 3a). Our simulation demonstrates that even if the strong electric field can cause the apparent orientation of dipolar H_2O molecules, the sign effect of ions can be still considerable, which results in an apparent disparity in solvation energies between cations and anions. The Born solvation energy (the green line in Fig. 3a) is often used to predict the solvation energy at different ionic sizes, yet it cannot sufficiently capture the solvation discrepancy between cations and anions, nor the alternations in solvation caused by the application of the electric fields. Here, the Born solvation energy of single ions in aqueous solutions is calculated as $\Delta G_{\text{Born}} = \frac{Z^2 e^2}{8\pi\varepsilon_0 R_i}(1/\varepsilon_r - 1)$, in which the dielectric constant of water is set to be 80.

In Fig. 4 and Fig. S2 (in ESI), we further investigate the detailed structure variations of H_2O near the ions under $\vec{E}$ by detecting the radial distribution functions of H and O (in H_2O) surrounding the ions. Our simulations illustrate that at the weak electric field, the H_2O molecules orient towards the ions and show significant affinity to the anions due to the strong anion-H electrostatic attractions [$g_{i(a)-O}(r)$ and $g_{i(a)-H}(r)$ in Figs. 4a and 4b]. In contrast, the H_2O molecules exhibit opposite orientations around cations, leading to the estrangement of H from ions [$g_{i(c)-O}(r)$ and $g_{i(c)-H}(r)$ in Figs. 4c and 4d]. The enlargement of ionic radii from Li^+/Li^- (σ_i=2.337 Å) to I^+/I^- (σ_i=4.168 Å) can significantly weaken the ion-H_2O affinity, which results in the decrease and shifting (towards larger r)

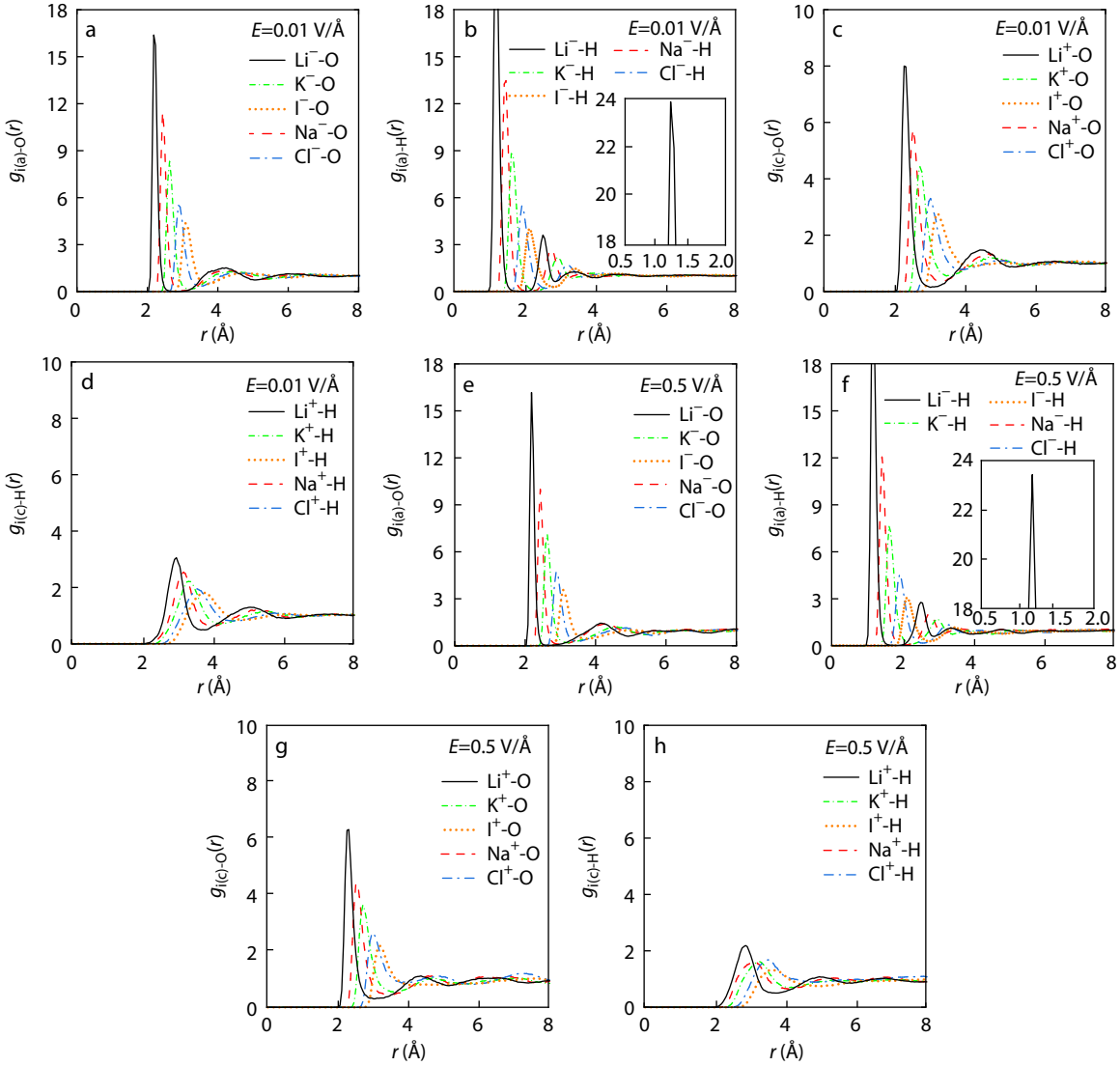

Fig. 4 Radial distribution functions for (a) O and (b) H (in H_2O) near each anion under an external electric field strength of E=0.01 V/Å, denoted as $g_{i(a)-O}(r)$ and $g_{i(a)-H}(r)$; Radial distribution functions for (c) O and (d) H (in H_2O) near each cation under an external electric field strength of E=0.01 V/Å, denoted as $g_{i(c)-O}(r)$ and $g_{i(c)-H}(r)$; (e, f) Correspond to the results of (a, b) at E=0.5 V/Å, respectively; (g, h) Correspond to the results of (c, d) at E=0.5 V/Å, respectively.

https://doi.org/10.1007/s10118-024-3105-9

the peak values of $g_{i-O}(r)$ and $g_{i-H}(r)$. Moreover, by increasing the electric field to E=0.5 V/Å, the exerted electric field causes the orientation of the H_2O molecules and suppresses their dipolar response towards the electrostatic field stemming from ions, which results in the decreased peak values in $g_{i-O}(r)$ and $g_{i-H}(r)$ (Figs. 4e–4h).

Overall, our simulations indicate that the ion solvations are sensitively dependent on the strength of the external electric field. At weak $\vec{E}$, we observe the significant discrepancy in solvation energies between cations/anions due to the reversal orientations of the asymmetric dipolar H_2O. However, by applying the strong $\vec{E}$, the ion solvation effects become weak and this discrepancy can be significantly shrunk. These results demonstrate that in studies for ion-containing liquid systems under external electric fields, the effect of asymmetric dipolar molecules in response to ions should be carefully considered; however, such effects are often neglected by theory and simulation studies with dielectric continuum. In our previous studies, we have utilized MD simulation algorithms developed based on the Stockmayer fluid model to explore the interactions of ion and dipolar liquid molecules under $\vec{E}$ and observe the similar decay of dipolar response of liquids towards ions caused by $\vec{E}$ application.[18] Our current work demonstrates that even under a strong electric field, the sign effect results in apparent discrepancies in solvating of cations and anions, which cannot be captured by the Stockmayer fluid model developed based on symmetric dipolar natures.

Structures of Ionic Solutions

By clarifying the impacts of applied electric fields on ion solvation in aqueous solutions, we further investigate the structures of ionic aqueous solutions. Herein, to emphasize the effects of electrostatic interactions, we only maintain the repulsive part in the LJ potential (Eq. 1) between ions and between ions and H_2O molecules.

We show the typical snapshots of K^+/I^- and K^-/I^+ ionic solutions with a concentration of 0.5 mol/L at different E in Figs. 5(a)–5(c), 5(e)–5(g), calculate the corresponding structure factors of ions in Figs. 5(d) and 5(h), and provide the radial distribution functions of O and H (in H_2O) near the ions in Fig. 6. We calculate the structure factor according to $S(q) = \frac{1}{N}\left\langle \sum_{j=1}^{N}\sum_{k=1}^{N} \exp\left[-i\mathbf{q}\cdot(\mathbf{r}_j - \mathbf{r}_k)\right]\right\rangle$, where N denotes

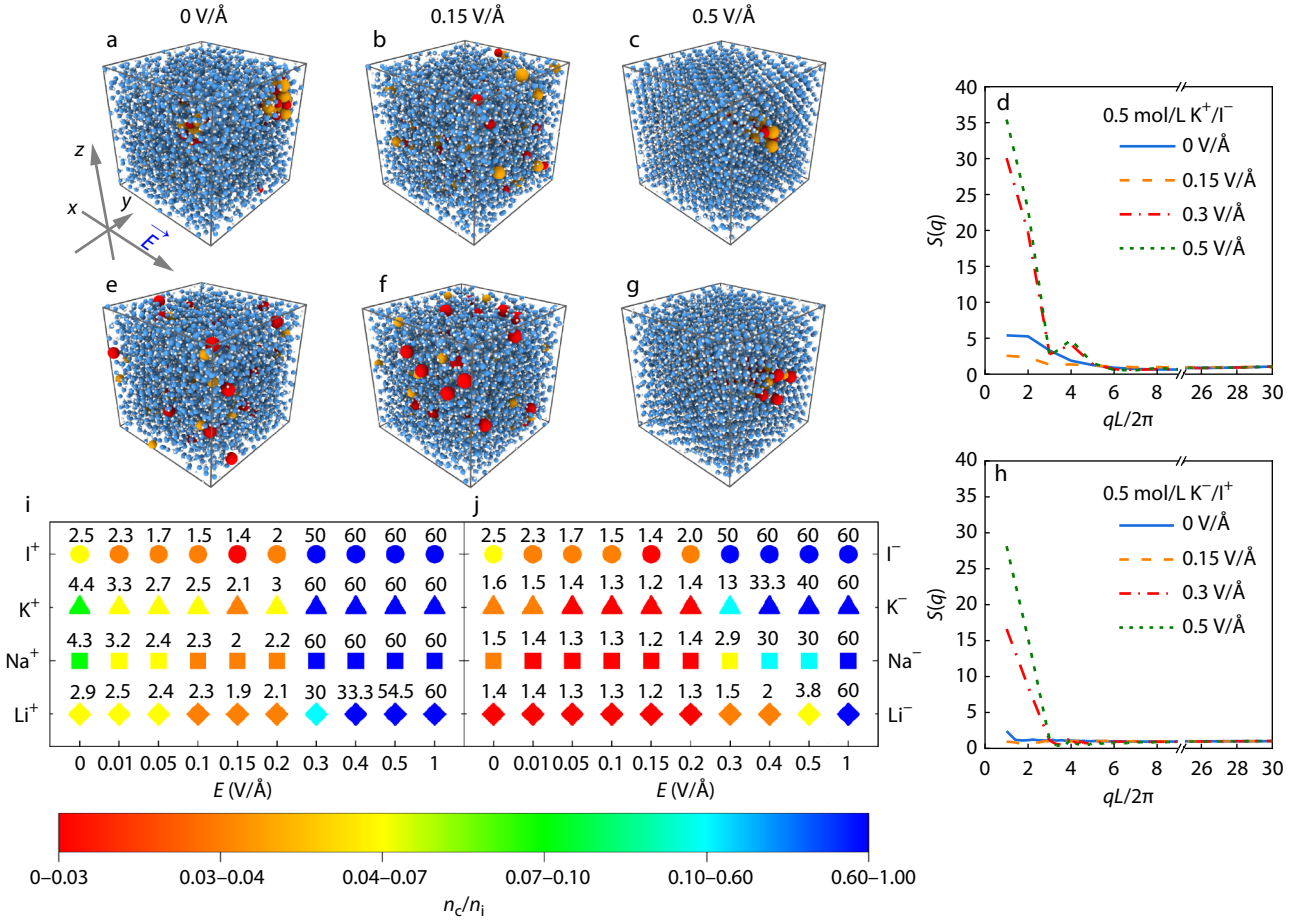

Fig. 5 Typical snapshots of K^+/I^- and K^-/I^+ ionic solutions at a concentration of 0.5 mol/L at different external electric field strengths: (a) E=0 V/Å, (b) E=0.15 V/Å, and (c) E=0.5 V/Å for K^+/I^- and (e) E=0 V/Å, (f) E=0.15 V/Å, and (g) E=0.5 V/Å for K^-/I^+ solutions. The red, orange, blue and white spheres represent cations, anions, O atoms, and H atoms, respectively, and the x-direction in the coordinate system of (a) corresponds to $\vec{E}$ direction. Structure factors of (d) K^+/I^- and (h) K^-/I^+ ionic clusters at different external electric field strengths. The reduced sizes (n_c/n_i) of (i) M^+/I^- and (j) M^-/I^+ (where M^+/M^- represents Li^+/Li^-, Na^+/Na^-, K^+/K^-, or I^+/I^-) ionic clusters at different electric field strengths, where n_c is the amount of ions in each cluster and n_i represents the amount of all ions.

https://doi.org/10.1007/s10118-024-3105-9

the total ion number, q indicates the wavenumber, and i represents the imaginary unit. $\mathbf{r}_j$ and $\mathbf{r}_k$ indicate the position vectors of the j^{th} and k^{th} ions, and <···> denotes the statistical average. Our simulation illustrates that, for the K^+/I^- ionic solutions, in the absence of the external electric field (E=0 V/Å), due to the relatively weak solvation effects of both K^+ cations and large I^- anions in the H_2O molecules (Fig. 6a), the electrostatic interactions of ions play the dominate role, causing the apparent ion clusterings in the aqueous solutions, as shown by the snapshot in Fig. 5(a) and peak value of $S(q)$ in Fig. 5(d). Contrastingly, for K^-/I^+ ionic solutions, due to the strong solvation of K^- anions (Fig. 6d), the ions disperse in the H_2O molecules, as illustrated by snapshot (Fig. 5e) as well as the relatively flat curve of $S(q)$ (Fig. 5h). With the electric field strength increasing to E=0.15 V/Å, in both the K^+/I^- and K^-/I^+ ionic solutions, the reversal electric forces exerted onto anions and cations conquer the electrostatic attractions between ions, and enhance their dispersion and affinity to the H_2O solvent molecules, as shown by the snapshots in Figs. 5(b), 5(d), 5(f) and 5(h) and Figs. 6(b) and 6(e). Particularly, in the K^+/I^- ionic solutions, we observe the complete disassembly of ionic clusters and sufficient ion solvation by the H_2O molecules. Furthermore, our simulation shows that at $E \sim 0.5$ V/Å, the strong electric force causes the complete orientation of dipolar H_2O molecules, thereby weakening the dipole response capability of water molecules to ions and resulting in a reduction of ion solvation effects. In this context, the system exhibits the dielectric decrement effect, leading to the formation of dynamic aggregate structures between anionic and cationic components in both the K^+/I^- and K^-/I^+ ionic solutions through electrostatic interactions, as shown by the snapshots in Figs. 5(c), 5(d), 5(g) and 5(h) and Figs. 6(c) and 6(f). Moreover, we observe that the cations and anions (undertaking the opposite electric forces) constantly diffuse in opposite directions within the aggregates or migrate into the other ionic aggregates. The cations and anions exhibit convections within the ion-rich regions along the electric field directions.

Further, we analyze the ionic clusters in the solutions at different electric field strengths. To identify ionic clusters, we group ions within a cutoff distance of 1.5σ (σ=4.168 Å) and calculate the average number of ions in each cluster (n_c) as $n_c = \left\langle \sum_{j=1}^{n_i} n_c^j P\left(n_c^j\right) \right\rangle$, where $P\left(n_c^j\right)$ is the cluster size distribution function defined as $P\left(n_c^j\right) = \left\langle q\left(n_c^j\right)\right\rangle / \sum_{j=1}^{n} \left\langle q\left(n_c^j\right)\right\rangle$, and $q\left(n_c^j\right)$ denotes the number of n_c^j clusters. In Figs. 5(i) and 5(j), we show the reduced size of M^+/I^- and M^-/I^+ ionic clusters (where M^+/M^- represents Li^+/Li^-, Na^+/Na^-, K^+/K^-, or I^+/I^-), calculated as n_c/n_i, where n_i indicates the amount of all ions. Our study indicates that for both the M^+/I^- and M^-/I^+ solutions, with increasing E, the size of the ionic cluster exhibits non-monotonic variations. At the weak electric field region $E \leq 0.3$ V/Å, the increase of E strengthens the opposite electric force exerting on the cations and anions, and results in their dissociations. At the strong electric field region E>0.3 V/Å, increasing E restricts H_2O orientations, which significantly weakens the ion solvation and results in their aggregations. Note that

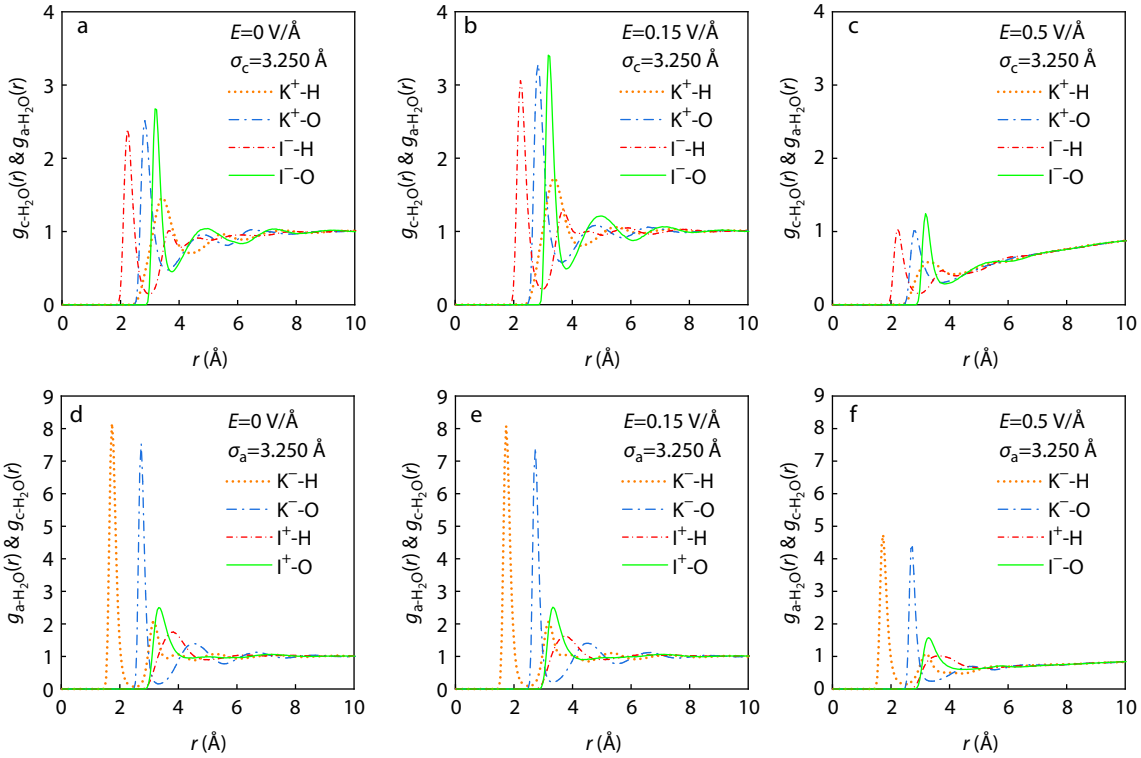

Fig. 6 Radial distribution functions for O and H (in H_2O) near K^+ and I^- in 0.5 mol/L K^+/I^- ionic solution under external electric field strengths of (a) E=0 V/Å, (b) E=0.15 V/Å and (c) E=0.5 V/Å, denoted as $g_{c\text{-}H_2O}(r)$ and $g_{a\text{-}H_2O}(r)$. Radial distribution functions for O and H (in H_2O) near K^- and I^+ in 0.5 mol/L K^-/I^+ ionic solution under external electric field strengths of (d) E=0 V/Å, (e) E=0.15 V/Å and (f) E=0.5 V/Å, denoted as $g_{a\text{-}H_2O}(r)$ and $g_{c\text{-}H_2O}(r)$.

https://doi.org/10.1007/s10118-024-3105-9

these tendencies are consistent with our previous simulations study of multibody interactions between ions and symmetric dipolar molecules with larger dipole moments.[18] Moreover, we find that the cluster sizes in M^+/I^- and M^-/I^+ solutions are qualitatively different. Specifically, due to the relatively stronger solvation effect of M^- compared to the M^+, the ions in M^-/I^+ solutions exhibit more dispersed structures and form smaller ionic clusters than the M^+/I^- solutions, at relatively weak electric field E≤0.3 V/Å. It is worth noting that in charged systems, the translational entropy that usually causes the ion dispersion can compete with the enthalpy effect arising from the electrostatic interactions between ions, which together determine the size of ionic clusters.

In addition, our simulations show that increasing the ionic size can result in the enhancement of electrostatic interactions and the decay in the ionic solvations in water molecules, and the competition of these two effects can cause completely different variations in cluster sizes between M^+/I^- and M^-/I^+ solutions. For example, in the M^-/I^+ solutions, at fixed electric field strength (*e.g.*, E≤0.5 V/Å), with increasing the M^- size, the solvation effect of M^- anions are decayed, and therefore, the ions form larger ionic clusters through electrostatic interactions, which results in a monotonic increase in n_c/n_i. However, in the M^+/I^- solutions, the solvation effects of ions are relatively weak. At fixed electric field strength (*e.g.*, E≤0.5 V/Å), with increasing the M^+ size, n_c/n_i first exhibits an increase due to the prominence of electrostatic interactions (as the solvation effect is significantly weak), followed by a decrease due to the further attenuation or electrostatic interactions at much larger ionic size (at I^+). Our simulation thus demonstrates that the sign effect as well as dipolar asymmetry of liquids can cooperate with $\vec{E}$ to cause the apparent structural discrepancy between M^+/I^- and M^-/I^+ solutions, which have been largely ignored by the previous theoretical and simulation studies, even if the studies based on the multi-body correlations of ions and symmetric dipoles or dielectric continuity.

Structures of PE Solutions

In polyelectrolyte (PE) solutions, chain connectivities can greatly amplify the complexity of multi-body interactions between ionic species and dipoles. Moreover, the applied electric field can further alter these interactions. In this subsection, we turn to investigate the structures of anionic and cationic polyelectrolytes in aqueous solutions under the influence of an external electric field. As a typical example, we first focus on the PE solutions with an overlap concentration (at E=0 V/Å), of which the monomer concentration is estimated as $c_m^* \sim n_p/\left[4\pi\left(R_g\right)^3/3\right]$

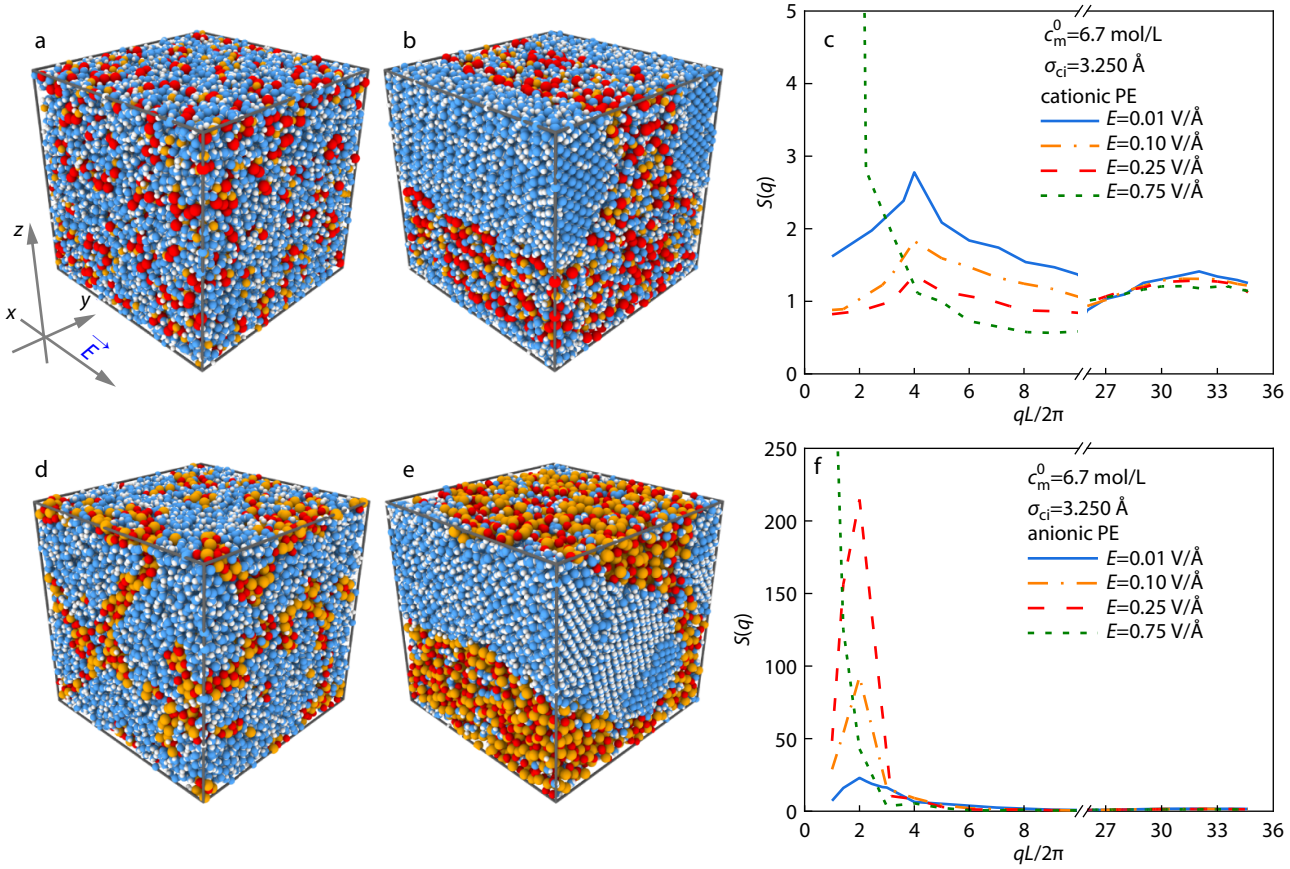

Fig. 7 Representative simulation snapshots of cationic PEs in aqueous solutions under external electric field strengths of (a) E=0.01 V/Å and (b) E=0.75 V/Å. The x-direction in the coordinate system of (a) corresponds to the direction of the electric field. Similarly, representative simulation snapshots of flexible anionic PEs under external electric field strengths of (d) E=0.01 V/Å and (e) E=0.75 V/Å. To highlight the structure of polyelectrolytes and counterions, the size of H_2O is reduced. Structure factors of (c) cationic or (f) anionic PEs and counterions in solutions under different external electric fields.

https://doi.org/10.1007/s10118-024-3105-9

~ 6.8 mol/L,[35] (n_p and R_g are the numbers and radius of gyration of the PE chains). Figs. 7(a), 7(b), 7(d) and 7(e) illustrate the representative simulation snapshots of anionic and cationic PEs in aqueous solutions, under an external electric field strength of (a) E=0.01 V/Å and (b) E=0.75 V/Å. The static structure factors of the PEs and counterions under different electric field strengths are presented in Figs. 7(c) and 7(f). In addition, in Fig. S3 (in ESI), we display the radial distribution functions for H and O (in H_2O) near each PE monomer and counterion. Our simulation demonstrates that the anionic and cationic PEs exhibit completely different structural variations under the electric field.

Specifically, in cationic PE solutions, at the weak electric field strength E = 0.01 V/Å, the relatively strong solvations of counteranions in aqueous solution cause their dissociations from PEs. In addition, the electrostatic repulsions of cationic monomers cause the extension of the PE chains. Therefore, the cationic PE chains exhibit a uniform distribution in the aqueous solution, as illustrated by the snapshots and flat curves of $S(q)$ in Figs. 7(a) and 7(c). With the increase in the electric field strength from E=0.01 V/Å to 0.25 V/Å, the reversal electric forces exerted onto cationic monomers and counteranions are increased. Meanwhile, the relatively strong solvation of ions still dominates over the structure of PEs and counterions. In this context, more counterions dissociate from the PEs, which further promotes the uniform dispersion of PEs, as shown by the decrease in the peak value of $S(q)$ in Fig. 7(c). However, with the further increase of E to 0.75 V/Å, the strong electric field arouses apparent H_2O orientating, which restricts their dipolar response to the ions and greatly weakens the ion solvation effect. In this context, the electrostatic attraction between cationic PEs and the counteranions dominates over the solvation effect, which results in the significant aggregation between the charged species, (snapshots and sharp upturn of $S(q)$ in Figs. 7b and 7c).

Contrastingly, for anionic PE solutions, at E=0.01 V/Å, because of the weak solvations of countercations. In this context, the electrostatic attractions of countercations and anionic PEs conquer their solvation effects. The countercations and anionic PEs exhibit microscopic aggregations in the solutions, (snapshots and apparent peak of $S(q)$ in Figs. 7d and 7f). Moreover, due to the weak solvation effect and the dominant impact of electrostatic attractions for ionic components, with the increase of E to 0.75 V/Å, the strengthened electric field can restrict the dipolar response of the H_2O to the ions. In this context, the electrostatic interactions thoroughly overwhelm the solvation effect, which results in the monotonically increased aggregation of the anionic PEs and countercations, as shown by the snapshots in Fig. 7(e) and the significant increase in peak value $S(q)$ at in Fig. 7(f).

Finally, the diagrams for structures of anionic and cationic PEs in aqueous solutions as a function of electric field strengths and monomer concentrations are summarized in Fig. 8. Our simulations indicate that the competition among electrostatic interactions, solvation of the PEs and counterions in H_2O molecules as well as the applied $\vec{E}$ can cause the formation of enriched structures of PE solutions. Specifically, at relatively weak electric field strength (E<0.5 V/Å), the cationic PEs exhibit ideal solubility and uniform distribution in aqueous solutions because of the strong solvation effects. In

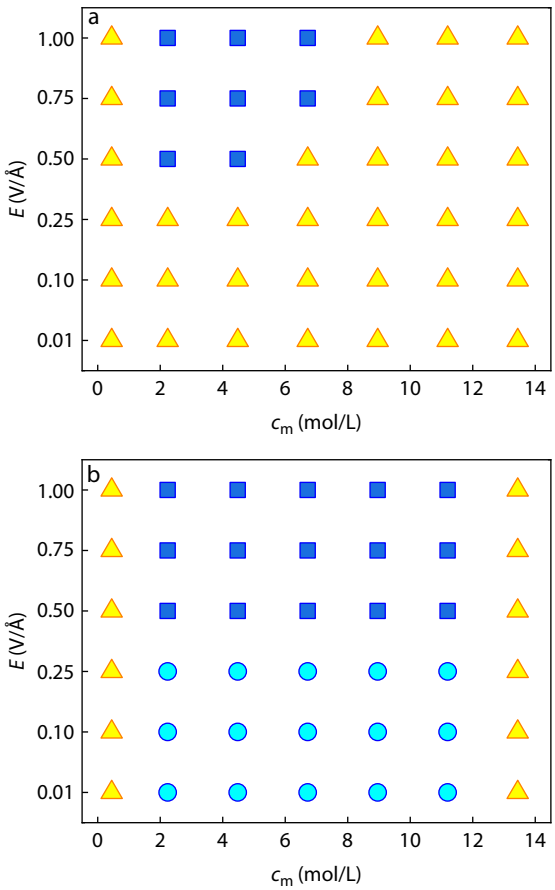

Fig. 8 Diagrams for structures of (a) cationic and (b) anionic PE solutions as a function of monomer concentrations (c_m) and external electric field strength (E). The dark blue square, light blue circle and yellow triangle denote the strong microscopic aggregation structure, weak microscopic aggregation structure and uniform solution state, respectively.

contrast, there exist weak aggregation regions for the anionic PEs due to the dominance of electrostatic interaction between ionic species. With increasing the electric field strength at E≥0.5 V/Å, the electric field can cause significant orientations of dipolar molecules as well as dielectric decrement of the solutions. In these conditions, the solvation effects of H_2O molecules are significantly weakened; therefore, the electrostatic interactions dominate over the system structures and the PE chains exhibit strong aggregations in the aqueous solution at the intermediate PE concentrations. It is worth noting that due to the relatively stronger solvation effect of counteranions, the strong aggregation region in cationic PE solutions is narrower than that in the anionic PE solutions. In addition, the extent of PE aggregation at c=2.2–11.2 mol/L exhibits a nonmonotonic increase with increasing the electric field strength, as illustrated in the discussion for Figs. 7(a)–7(c). It is noteworthy that previous experimental studies have indicated that a relatively weak external electric field can induce the aggregation of microscopic coacervate droplets composed of oppositely charged polyelectrolytes, leading to the formation of chain-like structures that further aggregate with the increase in electric field strength.[72] Additionally, in the experimental study on the external electric field-driven

self-assembly of ionic microgels, it has been observed that the ionic microgel particles form chain-like structures induced by the weak electric field, and with the increase in the electric field, further aggregation occurs between these chain-like structures.[73] The formation of these experimental phenomena is attributed to the enhanced dipolar nature of these droplets induced by the electric field. Importantly, our findings regarding the aggregation of PE chains under $\vec{E}$ are similar to these phenomena, and our simulations suggest that the dielectric decrement of the solvent could be another possible reason for the observed aggregations in experiments.

CONCLUSIONS

In summary, we investigate the structures of ions and polyelectrolytes in aqueous solutions under external electric fields using molecular dynamics simulations. We employ a coarse-grained model to simulate ionic species and use the TIP3P model to simulate the H_2O molecules. Our model can capture the alternations in multibody correlations between ions, polyelectrolytes, and asymmetric dipolar H_2O molecules stemming from the applications of external electric fields.

We first investigate the solvation of individual ions with different radii under the applied electric field. It is illustrated that even under the electric field, at fixed ionic radii, the reorienting H_2O molecules toward ions can cause nontrivial disparities in solvation effects between anions and cations, *i.e.*, anions retain much lower solvation energy than cations. With increasing the electric field strength, the electric fields can enhance the orientation of dipolar H_2O and restrict their dipolar response to ions, which results in the decay in ion solvation and diminished difference in solvation energies for anions and cations. The classical Born solvation energy, which is often used to predict the solvation energy at different ionic sizes, cannot sufficiently capture these variations in ion solvations, as well as the alternations of ions caused by the application of the electric field.

We then systematically study the structures of ionic solutions. Taking M^+/I^- and M^-/I^+ types of salt ions (where M^+/M^- represents the ions of which the size is identical to Li^+/Li^-, Na^+/Na^-, K^+/K^-, or I^+/I^-) as examples, we demonstrate that the reversal of charge sign can cause significant differences in ionic clustering, and the exerted electric field can further cause microstructural variations of ions in aqueous solutions. Specifically, on one hand, the electric field can exert reversal forces onto cations/anions and promote their dispersions; on the other hand, the electric fields restrict dipolar responses of H_2O and cause the dielectric decrement of the media, which in turn arouses the cation/anion aggregations. The competition of these effects results in the non-monotonic dependence of ionic cluster size on the electric field strength. In addition, due to the asymmetric dipolar nature of H_2O and the disparity in solvation effects for anions and cations, M^-/I^+ types of ions exhibit a more dispersed distribution compared to the M^+/I^- ions.

Based on the above findings, we further explore the structural properties of polyelectrolytes in aqueous solutions. It is indicated that anionic and cationic polyelectrolytes exhibit completely different architectures under electric fields. At weak electric field strength, the cationic polyelectrolytes exhibit a uniform distribution in water attributed to the dominant solvation effect of counteranions, the anionic polyelectrolyte tend to weakly aggregate due to their stronger electrostatic interactions with countercations. Because of the coupling of interactions between polyelectrolytes, counterions, and H_2O with the electric force, increasing the electric field can cause nonmonotonic variations in aggregation degree for cationic polyelectrolytes, but monotonic variations for anionic polyelectrolytes.

Attributed to the complex and long-range multi-body electrostatic interplays between dipolar and ionic components, the modeling of ion-containing polymers and soft matters remains challenging. The couplings between sign effects (induced by asymmetric dipolar natures) and electric force have been particularly disregarded in previous studies. Since most of the dipolar models, such as the Stockmayer fluid-like models could only consider the symmetric dipolar nature of the liquid molecules, it would be important to develop new theories and simulation algorithms that are capable of accounting for these effects. The sign effects can be significantly altered by the application of external fields, we propose that these effects should be carefully considered in the relative studies. In-depth and extensive experimental studies focusing on the sign effects of ionic and polyelectrolyte systems would also be necessary. Note that estimating the dielectric constant from the reoriented dipolar nature of the liquid molecules around ions is crucial for further understanding the structural and dynamic properties of ion-containing liquid materials.[20,42,43,74] Additionally, the application of electric field can result in a significant decrease in the dielectric constant of the ionic solution.[19,71] Therefore, it is essential to investigate the impacts of external electric fields and sign effects on the dielectric properties of the system. Moreover, in recent years, studies on terahertz technology have been attracting extensive attention.[75,76] It would be important to further explore the multi-body interactions between asymmetric dipolar solvents and ionic species under the terahertz alternating current electric fields.

Given that most polar solvents and some functional liquid additives[45] exhibit a typical asymmetric dipolar nature, we expect that the key findings and conclusions regarding the sign effects on structures of ionic and polyelectrolyte under an external electric field in this work might apply to many ionic complex liquids and biological systems. This study contributes to the comprehension of the fundamental physiochemical properties of ionic and polyelectrolyte solutions and brings insights into designing/developing relative materials.

Conflict of Interests

The authors declare no interest conflict.

Electronic Supplementary Information

Electronic supplementary information (ESI) is available free of charge in the online version of this article at http://doi.org/10.1007/s10118-024-3105-9.

Data Availability Statement

The data that support the findings of this study are available from the corresponding authors upon reasonable request. The authors' contact information: hfli@ciac.ac.cn (H.L.), xzduan@ciac.ac.cn (X.Z.D.).

ACKNOWLEDGMENTS

This work was financially supported by the Major Science and Technology Projects for Independent Innovation of China FAW Group Co., Ltd. (No. 20220301018GX), the National Natural Science Foundation of China (Nos. 9237210012, 22073094 and 21474109), the Science and Technology Development Program of Jilin Province (Nos. 20240602003RC and 20210402059GH), the State Key Laboratory of Molecular Engineering of Polymers (Fudan University) (No. K2023-08) and the Program for Young Scholars in Regional Development of CAS. We are grateful for the essential support of the Network and Computing Center, CIAC, CAS, and the Computing Center of Jilin Province.

REFERENCES

1 Muthukumar, M. *Physics of charged macromolecules synthetic and biological systems*. Cambridge University Press, **2023**.
2 Zhang, Z.; Chen, Q.; Colby, R. H. Dynamics of associative polymers. *Soft Matter* **2018**, *14*, 2961–2977.
3 Dobrynin, A. V.; Rubinstein, M. Theory of polyelectrolytes in solutions and at surfaces. *Prog. Polym. Sci.* **2005**, *30*, 1049–1118.
4 Dobrynin, A. V. Theory and simulations of charged polymers: from solution properties to polymeric nanomaterials. *Curr. Opin. Colloid Interface Sci.* **2008**, *13*, 376–388.
5 Sing, C. E.; Zwanikken, J. W.; Olvera de la Cruz, M. Electrostatic control of block copolymer morphology. *Nat. Mater.* **2014**, *13*, 694–698.
6 Shen, K.; Wang, Z. G. Electrostatic correlations and the polyelectrolyte self energy. *J. Chem. Phys.* **2017**, *146*, 084901.
7 Friedowitz, S.; Salehi, A.; Larson, R. G.; Qin, J. Role of electrostatic correlations in polyelectrolyte charge association. *J. Chem. Phys.* **2018**, *149*, 163335.
8 Brown, J. R.; Seo, Y.; Hall, L. M. Ion correlation effects in salt-doped block copolymers. *Phys. Rev. Lett.* **2018**, *120*, 127801.
9 Hao, Q. H.; Xia, G.; Miao, B.; Tan, H. G.; Niu, X. H.; Liu, L. Y. Morphological response of a spherical polyelectrolyte brush to solvent quality and electrostatic interaction strength. *Macromolecules* **2018**, *51*, 8513–8521.
10 Liu, L.; Wang, F.; Liu, X.; Guo, L.; Gao, X.; Tan, H. Self-assembly of amphiphilic polyelectrolytes in trivalent salt solution. *Phys. Chem. Chem. Phys.* **2023**, *25*, 10042–10053.
11 Fong, K. D.; Self, J.; McCloskey, B. D.; Persson, K. A. Ion correlations and their impact on transport in polymer-based electrolytes. *Macromolecules* **2021**, *54*, 2575–2591.
12 Debye, P. *Polar molecules*. Chemical Catalog Co., New York, **1929**.
13 Wang, Z. G. Effects of ion solvation on the miscibility of binary polymer blends. *J. Phys. Chem. B* **2008**, *112*, 16205–16213.
14 Levy, A.; Andelman, D.; Orland, H. Dielectric constant of ionic solutions: a field-theory approach. *Phys. Rev. Lett.* **2012**, *108*, 227801.
15 Gong, H.; Freed, K. F. Langevin-Debye model for nonlinear electrostatic screening of solvated ions. *Phys. Rev. Lett.* **2009**, *102*, 057603.
16 Duan, X.; Nakamura, I. A new lattice Monte Carlo simulation for dielectric saturation in ion-containing liquids. *Soft Matter* **2015**, *11*, 3566–3571.
17 Onsager, L. Electric moments of molecules in liquids. *J. Am. Chem. Soc.* **1936**, *58*, 1486–1493.
18 Liang, J.; Wei, H.; Yu, K.; Lin, C.; Li, H.; Ding, M.; Duan, X. Structure and dynamics of ions in dipolar solvents: a coarse-grained simulation study. *Soft Matter* **2021**, *17*, 6305–6314.
19 Booth, F. The dielectric constant of water and the saturation effect. *J. Chem. Phys.* **1951**, *19*, 391–394.
20 Daniels, I. N.; Wang, Z.; Laird, B. B. Dielectric properties of organic solvents in an electric field. *J. Phys. Chem. C* **2017**, *121*, 1025–1031.
21 Rezaei, M.; Mitterwallner, B. G.; Loche, P.; Uematsu, Y.; Netz, R. R.; Bonthuis, D. J. Interfacial, electroviscous, and nonlinear dielectric effects on electrokinetics at highly charged surfaces. *J. Phys. Chem. B* **2021**, *125*, 4767–4778.
22 Huo, H.; Zhao, W.; Duan, X.; Sun, Z. Y. Control of diblock copolyelectrolyte morphology through electric field application. *Macromolecules* **2023**, *56*, 1065–1076.
23 Herrera, S. E.; Agazzi, M. L.; Apuzzo, E.; Cortez, M. L.; Marmisolle, W. A.; Tagliazucchi, M.; Azzaroni, O. Polyelectrolyte-multivalent molecule complexes: physicochemical properties and applications. *Soft Matter* **2023**, *19*, 2013–2041.
24 Fang, Y. N.; Rumyantsev, A. M.; Neitzel, A. E.; Liang, H.; Heller, W. T.; Nealey, P. F.; Tirrell, M. V.; de Pablo, J. J. Scattering evidence of positional charge correlations in polyelectrolyte complexes. *Proc. Natl. Acad. Sci. U.S.A.* **2023**, *120*, e2302151120.
25 Ylitalo, A. S.; Balzer, C.; Zhang, P.; Wang, Z. G. Electrostatic correlations and temperature-dependent dielectric constant can model LCST in polyelectrolyte complex coacervation. *Macromolecules* **2021**, *54*, 11326–11337.
26 Chen, S.; Zhang, P.; Wang, Z. G. Complexation between oppositely charged polyelectrolytes in dilute solution: effects of charge asymmetry. *Macromolecules* **2022**, *55*, 3898–3909.
27 Zhang, P.; Wang, Z. G. Supernatant phase in polyelectrolyte complex coacervation: cluster formation, binodal, and nucleation. *Macromolecules* **2022**, *55*, 3910–3923.
28 Wang, L.; Wang, Z.; Jiang, R.; Yin, Y.; Li, B. Conformation transitions of a single polyelectrolyte chain in a poor solvent: a replica-exchange lattice Monte-Carlo study. *Soft Matter* **2017**, *13*, 2216–2227.
29 Zhu, Y. L.; Lu, Z. Y.; Milano, G.; Shi, A. C.; Sun, Z. Y. Hybrid particle-field molecular dynamics simulation for polyelectrolyte systems. *Phys. Chem. Chem. Phys.* **2016**, *18*, 9799–9808.
30 Wang, R.; Ginzburg, V. V.; Jiang, J.; Wang, Z. G. Adsorption of a polyelectrolyte chain at dielectric surfaces: effects of surface charge distribution and relative dielectric permittivity. *Macromolecules* **2023**, *56*, 7653–7662.
31 Chen, X.; Chen, E. Q.; Shi, A. C.; Yang, S. Multiphase coacervates driven by electrostatic correlations. *ACS Macro Lett.* **2021**, *10*, 1041–1047.
32 Yang, Z.; Wu, J.; Li, K.; Zhou, X.; Lu, D.; Zhang, L. Sliding dynamics of a small charged ring chain on the diblock polyelectrolyte in poly[2]catenane in the presence of counterions. *J. Phys. Chem. B* **2023**, *127*, 10189–10200.
33 Han, Y.; Zhao, X.; Liu, Y.; Li, Y.; Chen, Q. Structure and phase behavior of poly(acrylic acid)-ferric ion complex aqueous solutions. *Soft Matter* **2020**, *16*, 10750–10758.
34 Wu, S.; Yang, H.; Chen, Q. Improving stretchability of associative polymers through tuning density of the secondary interactions. *J. Rheol.* **2023**, *67*, 293–304.
35 Duan, X.; Shi, A. C.; An, L. Formation of ionomer microparticles *via* polyelectrolyte complexation. *Macromolecules* **2021**, *54*, 9053–9062.
36 Li, B.; Duan, X.; Cheng, D.; Chen, X.; Gao, Z.; Ren, W.; Shao, K.; Zang, H. Controllable transition metal-directed assembly of $[Mo_2O_2S_2]^{2+}$ building blocks into smart molecular humidity-responsive actuators. *J. Am. Chem. Soc.* **2023**, *145*, 2243–2251.
37 Liu, B.; Hu, B.; Du, J.; Cheng, D.; Zang, H.; Ge, X.; Tan, H.; Wang, Y.; Duan, X.; Jin, Z.; Zhang, W.; Li, Y.; Su, Z. Precise molecular-level modification of nafion with bismuth oxide clusters for high-

performance proton-exchange membranes. *Angew. Chem. Int. Ed.* **2021**, *60*, 6076–6085.
38 Yao, L.; Lin, C.; Duan, X.; Ming, X.; Chen, Z.; Zhu, H.; Zhu, S.; Zhang, Q. Autonomous underwater adhesion driven by water-induced interfacial rearrangement. *Nat. Commun.* **2023**, *14*, 6563.
39 Chen, L.; Zhao, C.; Duan, X.; Zhou, J.; Liu, M. Finely tuning the lower critical solution temperature of ionogels by regulating the polarity of polymer networks and ionic liquids. *CCS Chem.* **2022**, *4*, 1386–1396.
40 Shen, X.; Zhang, Y.; He, H.; Yi, C.; Dong, W.; Ye, S.; Zheng, D.; Tao, J.; Wu, Q.; Duan, X.; Nie, Z. Electrostatic adsorption behaviors of charged polymer-tethered nanoparticles on oppositely charged surfaces. *Macromol. Rapid Commun.* **2022**, *43*, 2200171.
41 Zhang, Y.; Yi, C.; Dong, W.; Zheng, D.; Yang, Y.; Li, W.; Duan, X.; Yang, D.; Nie, Z. Single copolymer chain-templated synthesis of ultrasmall symmetric and asymmetric silica-based nanoparticles. *Adv. Funct. Mater.* **2022**, *32*, 2112742.
42 Zhang, Q.; He, X. H. Phase separation of polymer blends induced by an external static electric field. *Chinese J. Polym. Sci.* **2023**, *41*, 972–980.
43 Zhang, Q.; Xu, R.; Kan, D.; He, X. Molecular dynamics simulation of electric-field-induced self-assembly of diblock copolymers. *J. Chem. Phys.* **2016**, *144*, 234901.
44 Balzer, C.; Frischknecht, A. L. Explicit polarization in Coarse-Grained simulations of ionomer melts. *Macromolecules* **2022**, *55*, 9980–9989.
45 Zhu, Z.; Duan, X.; Li, Q.; Wu, R.; Wang, Y.; Li, B. Low-noise nanopore enables in-situ and label-free tracking of a trigger-induced DNA molecular machine at the single-molecular level. *J. Am. Chem. Soc.* **2020**, *142*, 4481–4492.
46 Wang, Z.; Liang, S.; Yang, Y.; Liu, Z.; Duan, X.; Li, X.; Liu, T.; Zang, H. Complex phase transitions and phase engineering in the aqueous solution of an isopolyoxometalate cluster. *Nat. Commun.* **2023**, *14*, 2767.
47 Wilson, C. T. R. Condensation of water vapour in the presence of dust-free air and other gases. *Philos. Trans. R. Soc. Lond. A* **1897**, *189*, 265–307.
48 Loeb, L. B.; Kip, A. F.; Einarsson, A. W. On the nature of ionic sign preference in C. T. R. Wilson Cloud Chamber Condensation Experiments. *J. Chem. Phys.* **1938**, *6*, 264.
49 Oh, K. J.; Gao, G. T.; Zeng, X. C. Nucleation of water and methanol droplets on cations and anions: the sign preference. *Phys. Rev. Lett.* **2001**, *86*, 5080–5083.
50 Russell, K. C. Nucleation on gaseous ions. *J. Chem. Phys.* **1969**, *50*, 1809.
51 Talanquer, V.; Oxtoby, D. W. Nucleation in molecular and dipolar fluids: interaction site model. *J. Chem. Phys.* **1995**, *103*, 3686–3695.
52 Kusaka, I.; Wang, Z. G.; Seinfeld, J. H. Ion-induced nucleation: a density functional approach. *J. Chem. Phys.* **1995**, *102*, 913–924.
53 Kusaka, I.; Wang, Z. G.; Seinfeld, J. H. Ion-induced nucleation. II. Polarizable multipolar molecules. *J. Chem. Phys.* **1995**, *103*, 8993–9009.
54 Lin, C.; Wei, H.; Li, H.; Duan, X. Structures of cationic and anionic polyelectrolytes in aqueous solutions: the sign effect. *Soft Matter* **2022**, *18*, 1603–1616.
55 Price, D. J.; Brooks, C. L. A modified TIP3P water potential for simulation with Ewald summation. *J. Chem. Phys.* **2004**, *121*, 10096–10103.
56 A. D. MacKerell, J.; Bashford, D.; Bellott, M.; R. L. Dunbrack, J.; Evanseck, J. D.; Field, M. J.; Fischer, S.; Gao, J.; Guo, H.; Ha, S.; Joseph-McCarthy, D.; Kuchnir, L.; Kuczera, K.; Lau, F. T. K.; Mattos, C.; Michnick, S.; Ngo, T.; Nguyen, D. T.; Prodhom, B.; W. E. Reiher, I.; Roux, B.; Schlenkrich, M.; Smith, J. C.; Stote, R.; Straub, J.; Watanabe, M.; Wio´rkiewicz-Kuczera, J.; Yin, D.; Karplus, M. All-Atom Empirical Potential for Molecular Modeling and Dynamics Studies of Proteins. *J. Phys. Chem. B* **1998**, *102*, 3586–3616.
57 Jorgensen, W. L.; Chandrasekhar, J.; Madura, J. D.; Impey, R. W.; Klein, M. L. Comparison of simple potential functions for simulating liquid water. *J. Chem. Phys.* **1983**, *79*, 926–935.
58 Dang, L. X. Mechanism and thermodynamics of ion selectivity in aqueous solutions of 18-crown-6 ether a molecular dynamics study. *J. Am. Chem. Soc.* **1995**, *117*, 6954–6960.
59 Koneshan, S.; Rasaiah, J. C.; Lynden-Bell, R. M.; Lee, S. H. Solvent structure, dynamics, and ion mobility in aqueous solutions at 25 °C. *J. Phys. Chem. B* **1998**, *102*, 4193–4204.
60 Dang, L. X. Development of nonadditive intermolecular potentials using molecular dynamics: solvation of Li^+ and F^- ions in polarizable water. *J. Chem. Phys.* **1992**, *96*, 6970–6977.
61 Dang, L. X.; Smith, D. E. Molecular dynamics simulations of aqueous ionic clusters using polarizable water. *J. Chem. Phys.* **1993**, *99*, 6950–6956.
62 Dang, L. X.; Garrett, B. C. Photoelectron spectra of the hydrated iodine anion from molecular dynamics simulations. *J. Chem. Phys.* **1993**, *99*, 2972
63 Smith, D. E.; Dang, L. X. Computer simulations of NaCl association in polarizable water. *J. Chem. Phys.* **1994**, *100*, 3757
64 Nakamura, I.; Shi, A. C.; Wang, Z. G. Ion solvation in liquid mixtures: effects of solvent reorganization. *Phys. Rev. Lett.* **2012**, *109*, 257802.
65 Shock, C. J.; Stevens, M. J.; Frischknecht, A. L.; Nakamura, I. Solvation energy of ions in a stockmayer fluid. *J. Phys. Chem. B* **2020**, *124*, 4598–4604.
66 Hall, L. M.; Stevens, M. J.; Frischknecht, A. L. Dynamics of model Ionomer melts of various architectures. *Macromolecules* **2012**, *45*, 8097–8108.
67 Frenkel, D.; Smit, B. *Understanding molecular simulation: from algorithms to applications*. Academic, New York, **1996**.
68 Darden, T.; York, D.; Pedersen, L. Particle mesh Ewald: An N·log(N) method for Ewald sums in large systems. *J. Chem. Phys.* **1993**, *98*, 10089
69 Plimpton, S. Fast parallel algorithms for short-range molecular dynamics. *J. Comput. Phys.* **1995**, *117*, 1–19.
70 Nishida, K.; Kaji, K.; Kanaya, T. High concentration crossovers of polyelectrolyte solutions. *J. Chem. Phys.* **2001**, *114*, 8671–8677.
71 Hejazi, S.; Pahlavanzadeh, H.; Elliott, J. A. W. Thermodynamic investigation of the effect of electric field on solid-liquid equilibrium. *J. Phys. Chem. B* **2021**, *125*, 1271–1281.
72 Agrawal, A.; Douglas, J. F.; Tirrell, M.; Karim, A. Manipulation of coacervate droplets with an electric field. *Proc. Natl. Acad. Sci. U.S.A.* **2022**, *119*, e2203483119.
73 Colla, T.; Mohanty, P. S.; Nojd, S.; Bialik, E.; Riede, A.; Schurtenberger, P.; Likos, C. N. Self-assembly of ionic microgels driven by an alternating electric field: theory, simulations, and experiments. *ACS Nano* **2018**, *12*, 4321–4337.
74 Neumann, M. Dipole moment fluctuation formulas in computer simulations of polar systems. *Mol. Phys.* **1983**, *50*, 841–858.
75 Li, Y.; Chang, C.; Zhu, Z.; Sun, L.; Fan, C. Terahertz wave enhances permeability of the voltage-gated calcium channel. *J. Am. Chem. Soc.* **2021**, *143*, 4311–4318.
76 Ghalgaoui, A.; Fingerhut, B. P.; Reimann, K.; Elsaesser, T.; Woerner, M. Terahertz polaron oscillations of electrons solvated in liquid water. *Phys. Rev. Lett.* **2021**, *126*, 097401.